

FABRICATION OF TITANIUM DIOXIDE THIN
FILM PREPARED BY SPRAY PYROLYSIS
DEPOSITION METHOD FOR DYE-SENSITIZED
SOLAR CELL

FATIN IZYANI MOHAMAD FAZLI

UNIVERSITI TUN HUSSEIN ONN MALAYSIA

FABRICATION OF TITANIUM DIOXIDE THIN FILM PREPARED BY SPRAY
PYROLYSIS DEPOSITION METHOD FOR DYE-SENSITIZED SOLAR CELL

FATIN IZYANI MOHAMAD FAZLI

A thesis submitted in
fulfillment of the requirement for the award of the
Degree of Master in Electrical Engineering

Faculty of Electrical and Electronic Engineering
Universiti Tun Hussein Onn Malaysia

2017

This thesis was dedicated to my parents; Mohd Fazli Kamaruddin and Nor Aziah Ahmad, my siblings and my family

ACKNOWLEDGEMENT

I would like to express my earnest appreciation to my supervisor, Assoc. Prof. Dr. Mohd Khairul Ahmad, for his continuous support, encouragement and patience throughout this entire research work.

Special thanks are given to Microelectronics & Nanotechnology - Shamsuddin Research Centre (MiNT-SRC), Universiti Tun Hussein Onn Malaysia (UTHM) for aiding in technical and financial support. I would also like to acknowledge all MiNT-SRC technicians, Mrs. Faezahana and Ms. Isrihetty, my friends and labmates, Mrs. Sakinah, Mrs. Kamalia, Ms. Asyikin, Salina, Luqman, Kim Seng and Liyana for showing me the ropes and sharing their knowledge. I would also like to express my thankfulness for understanding parents, siblings and family members for always supporting me all the way to the submission of this thesis.

Finally, I wish to express my deepest appreciation to Universiti Tun Hussein Onn Malaysia for the opportunity to further my studies and for giving me a place to learn and expand my knowledge.

.

ABSTRACT

Nanostructured Titanium dioxide (TiO_2) thin films with the area of 0.25cm^2 were successfully fabricated on Fluorine-doped tin oxide (FTO) substrate on glass for dye sensitized solar cell (DSSC) application using spray pyrolysis deposition (SPD) method. The performance of each sample depend on the surface morphology, structure and thickness of the samples. The TiO_2 thin film was fabricated using P25 TiO_2 nanopowder which is a combination of anatase and rutile structure, to have different thickness ranging from $5\ \mu\text{m}$ to $20\ \mu\text{m}$ by varying the TiO_2 colloidal solution of 5 ml, 10 ml, 15 ml and 20 ml to find the optimum thickness for DSSC application. Field Emission Scanning Electron Microscopy (FESEM) analysis on the samples showed that the 5 ml sample with thickness of $2.379\ \mu\text{m}$ is too thin that the FTO structure underneath is visible. The sample with the highest efficiency of 1.677 % and $2.633\ \text{mA}/\text{cm}^2$ J_{sc} is yielded by 10 ml sample. Further optimization for the annealing temperature is done by varying the annealing temperature from $300\ ^\circ\text{C}$ to $500\ ^\circ\text{C}$ at fixed annealing time of 3 hours. Optimized annealing temperature is $500\ ^\circ\text{C}$ with 3.42 % efficiency and $5.359\ \text{mA}/\text{cm}^2$ J_{sc} . The annealing time was also varied to from 1 hour to 24 hours. The structural analysis of the samples showed that the rutile structure increased as the annealing time increased. The optimum annealing time is proven to be 3 hours with 4.034 % efficiency and $5.937\ \text{mA}/\text{cm}^2$ J_{sc} . TiO_2 samples fabricated by using pure anatase structure were also analyzed and compared to the samples fabricated using P25. The annealing temperature for the pure anatase samples was varied from $300\ ^\circ\text{C}$ to $500\ ^\circ\text{C}$. The efficiency of the P25 is slightly higher than pure anatase TiO_2 which has the highest efficiency of 3.249 % annealed at $500\ ^\circ\text{C}$. The optimum TiO_2 is the one fabricated with the P25 TiO_2 powder annealed at $500\ ^\circ\text{C}$ for 3 hours with the ruthenium based N719 dye as sensitizers.

ABSTRAK

Filem nipis nanostruktur TiO₂ dengan kawasan 0.25cm² telah berjaya dihasilkan di atas substrat FTO di atas kaca untuk aplikasi sel solar peka pewarna (DSSC) menggunakan kaedah semburan pirolisis (SPD). Prestasi setiap sampel bergantung kepada permukaan morfologi, struktur dan ketebalan sampel. Filem nipis TiO₂ telah dihasilkan menggunakan serbuk nano TiO₂ P25 yang merupakan gabungan struktur anatase dan rutil, untuk mempunyai ketebalan yang berbeza dari 5µm hingga 20µm dengan mengubah isipadu koloid TiO₂; 5 ml, 10 ml, 15 ml dan 20 ml untuk mencari ketebalan yang optimum bagi aplikasi DSSC. Analisis FESEM ke atas sampel menunjukkan bahawa sampel 5 ml dengan ketebalan 2.379 µm adalah terlalu nipis sehingga struktur FTO di bawahnya boleh dilihat. Sampel optimum adalah sampel 10 ml dengan kecekapan 1.677 % dan 2.633 mA/cm² *Jsc*. Proses optimum tambahan bagi suhu penyepuhlindapan dilakukan dengan mengubah suhu penyepuhlindapan daripada 300 °C ke 500 °C dengan masa penyepuhlindapan tetap selama 3 jam. Suhu penyepuhlindapan optimum adalah 500 °C dengan kecekapan 3.42 % dan *Jsc* 5.359 mA/cm². Masa penyepuhlindapan juga telah dikaji untuk 1 jam hingga 24 jam. Analisis struktur sampel menunjukkan bahawa struktur rutil meningkat jika masa penyepuhlindapan meningkat. Masa penyepuhlindapan optimum terbukti 3 jam dengan kecekapan 4.034 % dan 5.937 mA/cm² *Jsc*. Sampel TiO₂ juga dihasilkan dengan menggunakan struktur anatase tulen dan dianalisis serta dibandingkan dengan sampel yang dihasilkan menggunakan P25. Suhu penyepuhlindapan bagi sampel anatase diubah daripada 300 °C ke 500 °C. Kecekapan sampel P25 adalah lebih tinggi daripada anatase TiO₂ tulen yang menghasilkan kecekapan 3.249 %. TiO₂ optimum adalah yang dihasilkan dengan serbuk TiO₂ P25 disepuhlindap pada 500 °C selama 3 jam dengan pewarna berdasarkan ruthenium N719 sebagai pemeka.

TABLE OF CONTENTS

	DECLARATION	ii
	DEDICATION	iii
	ACKNOWLEDGEMENT	iv
	ABSTRACT	v
	ABSTRAK	vi
	TABLE OF CONTENTS	vii
	LIST OF TABLES	x
	LIST OF FIGURES	xi
	LIST OF SYMBOLS AND ABBREVIATIONS	xiv
	LIST OF APPENDICES	xv
	LIST OF PUBLICATIONS	xvi
CHAPTER 1	INTRODUCTION	1
	1.1. Solar cell technology	1
	1.2. Background of study	3
	1.3. Problem statement	5
	1.4. Hypothesis	5
	1.5. Objectives	6
	1.6. Project scopes	6
CHAPTER 2	LITERATURE REVIEW	7
	2.1. Dye sensitized solar cell (DSSC)	7
	2.2. Transparent conducting oxide (TCO)	10
	2.3. Dye sensitizers	11
	2.3.1. Synthetic dyes	11
	2.3.2. Organic dyes	13
	2.4. Electrolytes	14
	2.5. Counter electrode	15
	2.6. Titanium dioxide nanostructures	16

2.7.	Fabrication method	18
2.7.1.	Spray pyrolysis deposition (SPD) method	20
2.8.	Summary	23
CHAPTER 3	METHODOLOGY	24
3.1.	Substrate preparation	24
3.2.	TiO ₂ solution	26
3.2.1.	Varying TKC-303 solution & pure anatase TiO ₂ (Sigma-Aldrich)	27
3.3.	Deposition of TiO ₂ thin films	28
3.4.	Annealing of TiO ₂ thin films	28
3.5.	Dye and electrolyte preparations	29
3.6.	DSSC assembly	30
3.7.	Characterization of TiO ₂ thin film	32
3.7.1.	Field emission scanning electron microscopy (FESEM)	32
3.7.2.	X-ray diffractometer (XRD)	33
3.7.3.	Solar simulator	34
3.7.4.	UV-Vis spectrophotometer	36
3.8.	Summary	37
CHAPTER 4	RESULTS AND DISCUSSION	38
4.1.	Effect of varying thickness to the optical and structural properties of TiO ₂ thin films and its performance in a DSSC	38
4.1.1.	Surface morphology	38
4.1.2.	Thickness	41
4.1.3.	Optical properties	41
4.1.4.	Structural analysis	43
4.1.5.	Power conversion efficiency measurement	45
4.2.	Effect of annealing temperature on the structural properties of TiO ₂ thin films and its performance in a DSSC	46
4.2.1.	Surface morphology	47
4.2.2.	Structural analysis	49
4.2.3.	Power conversion efficiency measurement	50
4.3.	Effect of annealing time on the structural properties of TiO ₂ thin films and its performance in a DSSC	52

4.3.1.	Surface morphology	52
4.3.2.	Structural analysis	55
4.3.3.	Power conversion efficiency measurement	56
4.4.	Effect of annealing temperature on the structural properties of TiO ₂ thin films and its performance in a DSSC using pure anatase TiO ₂ (Sigma-aldrich, anatase > 99.7 %)	58
4.4.1.	Surface morphology	58
4.4.2.	Structural analysis	60
4.4.3.	Power conversion efficiency measurement	62
4.5.	Summary	64
CHAPTER 5	CONCLUSION	65
5.1.	Conclusion	65
5.2.	Future works	66
	REFERENCES	67
	APPENDIX	74
	VITAE	75

LIST OF TABLES

4.1	Crystallite size of TiO ₂ thin film based on different volume of TKC.	44
4.2	I-V measurements of DSSC using TiO ₂ thin film with different volume of TKC.	46
4.3	Crystallite size of TiO ₂ thin film based on different annealing temperature.	50
4.4	I-V measurements of DSSC with TiO ₂ samples annealed at different temperatures.	52
4.5	Crystallite size of TiO ₂ thin film based on different annealing time.	56
4.6	I-V measurements of DSSC with TiO ₂ samples annealed at different annealing time.	58
4.7	Crystallite size of TiO ₂ thin film (Sigma-Aldrich, anatase 99.7%) based on different annealing temperature.	61
4.8	I-V measurements of DSSC with TiO ₂ samples annealed at different temperatures.	64

LIST OF FIGURES

1.1	Generations of solar cell technology.	2
2.1	Layers of DSSC components.	8
2.2	A schematic diagram of a DSSC showing the principles of operation.	9
2.3	Structures of the ruthenium-based dyes N3, N719 and 'black dye' developed by the Grätzel group.	12
2.4	Structures of common anthocyanidins found in natural foods.	14
2.5	Classification of electrolytes for DSSC.	15
2.6	Unit cells of the TiO ₂ modifications rutile, brookite and anatase (from left to right).	17
2.7	TiO ₂ fabrication methods.	19
2.8	An illustration of spray pyrolysis deposition technique.	21
2.9	Illustration of the deposition process with increasing substrate temperature.	22
3.1	Flow chart of the methodology.	25
3.2	Flow chart of the FTO substrate cleaning process.	26
3.3	FTO substrate with aluminium mask.	26
3.4	(a) TiO ₂ solution grinded in a mortar. (b) Lightproof bottle with lid for ultrasonication.	27
3.5	(a) TiO ₂ deposition by SPD method. (b) Deposited TiO ₂ on masked and unmasked substrates.	28
3.6	TiO ₂ samples after annealing process in a furnace.	29
3.7	TiO ₂ immersed in dye.	30
3.8	(a) TiO ₂ photoanode and Pt counter electrode is clamped together on one side. (b) Electrolyte is inserted in between the electrodes through a dropper. (c) The electrodes are	31

	clamped on the other side to make a complete DSSC.	
3.9	Field Emission Electron Microcopy (FESEM).	32
3.10	Principle of X-Ray Diffraction Spectroscopy (XRD).	34
3.11	Solar Simulator.	35
3.12	UV-Visible Spectrophotometer (UV-Vis).	37
4.1	FESEM images of TiO ₂ with different amount of TKC (a) 5 ml, (b) 10 ml, (c) 15 ml and (d) 20 ml at 5, 000x magnification.	39
4.2	FESEM images of TiO ₂ with different amount of TKC (a) 5 ml, (b) 10 ml, (c) 15 ml and (d) 20 ml at 25, 000x magnification.	40
4.3	A graph of TKC-303 volume vs. TiO ₂ film thickness	41
4.4	Optical transmittance spectra of TiO ₂ films with (a) 20 ml TKC, (b) 15 ml TKC, (c) 10 ml TKC and (d) 5 ml TKC.	43
4.5	XRD pattern of TiO ₂ thin film with different volume of TKC.	44
4.6	Current density – voltage graph for the efficiency of DSSC using TiO ₂ thin film with different volume of TKC.	46
4.7	FESEM images of TiO ₂ (a) as deposited, and annealed at different temperatures (b) 300 °C, (c) 400 °C and (d) 500 °C at 5, 000x magnification.	47
4.8	FESEM images of TiO ₂ (a) as deposited, and annealed at different temperatures (b) 300 °C, (c) 400 °C and (d) 500 °C at 25, 000x magnification.	48
4.9	XRD spectra of TiO ₂ thin films annealed at different temperatures.	49
4.10	Current density – voltage graph of DSSC with TiO ₂ samples annealed at different temperatures.	51
4.11	FESEM images of TiO ₂ (a) as deposited, and annealed at different duration (b) 1 hour, (c) 3 hours, (d) 10 hours and (e) 24 hours at 5, 000x magnification.	53
4.12	FESEM images of TiO ₂ (a) as deposited, and annealed at different duration (b) 1 hour, (c) 3 hours, (d) 10 hours and	54

	(e) 24 hours at 25, 000x magnification.	
4.13	XRD spectra of TiO ₂ thin films annealed for different time duration.	55
4.14	Current density – voltage graph of DSSC with TiO ₂ samples annealed at different time durations.	57
4.15	FESEM images of TiO ₂ (Sigma-Aldrich) (a) as deposited and annealed at (b) 300 °C, (c) 400 °C and (d) 500 °C under 5,000x magnification.	59
4.16	FESEM images of TiO ₂ (Sigma-Aldrich) (a) as deposited and annealed at (b) 300 °C, (c) 400 °C and (d) 500 °C under 25, 000x magnification.	60
4.17	XRD pattern of TiO ₂ thin film using TiO ₂ anatase powder (Sigma-Aldrich, anatase 99.7%).	61
4.18	Current density – voltage graph of DSSC with TiO ₂ samples (Sigma-Aldrich, anatase 99.7%) annealed at different temperatures.	63
4.19	Comparison of current density – voltage graph of DSSC with TiO ₂ samples using pure anatase and P25 nanopowder annealed at different temperatures.	63

LIST OF SYMBOLS AND ABBREVIATIONS

AgBr	-	Silver bromide
AgCl	-	Silver chloride
CdTe	-	Cadmium telluride
CIGS	-	Copper indium gallium selenide
Cu ₂ O	-	Copper oxide
CVD	-	Chemical vapor deposition
DMPII	-	1,2-dimethyl-3-propyl-imidazolium iodide
DSSC	-	Dye sensitized solar cell
FESEM	-	Field Emission Scanning Electron Microscopy
FF	-	Fill factor
FTO	-	Fluorine doped tin oxide
<i>J_{sc}</i>	-	Current density
Nb ₂ O ₅	-	Niobium pentoxide
Pt	-	Platinum
Ru	-	Ruthenium
SnO ₂	-	Tin oxide
SPD	-	Spray pyrolysis deposition
TCO	-	Transparent conducting oxide
TiO ₂	-	Titanium Dioxide
UV-Vis	-	Ultraviolet-Visible Spectrophotometer
<i>V_{oc}</i>	-	Open circuit Voltage
XRD	-	X-ray Diffraction
ZnO	-	Zinc oxide
η	-	Power conversion efficiency

LIST OF APPENDICES

APPENDIX	TITLE	PAGE
A.1	Gantt chart of Research Activities	60

LIST OF PUBLICATIONS

- 1 Fatin Izyani Mohd Fazli**, Nafarizal Nayan, Mohd Khairul Ahmad, Noor Sakinah Khalid, Noor Kamalia Abd Hamed, Muhammad Luqman Mohd Napi. “Effect of Annealing Temperature on TiO₂ Thin Film Prepared by Spray Pyrolysis Deposition Method.” Proceeding of Conference on Nano-& Biosource Technology 2015 (NBT 2015), UKM Bangi, Selangor, 28-29 February 2015 (Sains Malaysiana Volume 45, No. 8 (August 2016), pg. 1197 – 1200).
- 2 Fatin Izyani Mohd Fazli**, Ahmad Naim Suhaimi, Noor Sakinah Khalid, Noor Kamalia Abd Hamed, Muhammad Luqman Mohd Napi, Salina Mohamad Mokhtar, Ng Kim Seng, Nurfarina Zainal, Nafarizal Nayan, Soon Chin Fhong, Mohd Khairul Ahmad, Suriani Abu Bakar, Azmi Mohamed. “The Effects of Annealing Temperature on the Properties of Aluminium Doped Tin Oxide (Al/SnO₂) Thin Films Deposited by Spray Pyrolysis Deposition (SPD) Method” Proceeding of Malaysian Technical Universities Conference on Engineering and Technology 2015, KSL Resort Hotel, Johor Bharu, 11 October-13 October 2015, ARPN Journal of Engineering and Applied Sciences (JEAS).
- 3 Fatin Izyani Mohamad Fazli**, Soon Chin Fhong, Nafarizal Nayan, Suriani Abu Bakar, Azmi Mohamed, Mohamad Hafiz Mamat, Mohd Firdaus Malek, Masaru Shimomura, Kenji Murakami. “Dye-sensitized Solar Cell using Pure Anatase TiO₂ Annealed at Different Temperatures” Optik – International Journal for Light and Electron Optics. (Accepted)
- 4** Noor Kamalia Abd Hamed, Nafarizal Nayan, Mohd Khairul Ahmad, Noor Sakinah Khalid, **Fatin Izyani Mohd Fazli**, Muhammad Luqman Mohd Napi. “Influence of Hydrochloric Acid Volume on Titanium Dioxide (TiO₂) Thin Film by Using Hydrothermal Method.” Proceeding of Conference on Nano-& Biosource Technology 2015 (NBT 2015), UKM Bangi, Selangor, 28-29

- February 2015 (Sains Malaysiana Volume 45, No. 11 (November 2016), pg. 1669–1673).
- 5 Noor Sakinah Khalid, **Fatin Izyani Mohd Fazli**, Noor Kamalia Abd Hamed, Muhammad Luqman Mohd Napi, Chin Fhong Soon, Mohd Khairul Ahmad. “Biocompatibility of TiO₂ Nanorods and Nanoparticles on Hela Cells.” Proceeding of Conference on Nano-& Biosource Technology 2015 (NBT 2015), UKM Bangi, Selangor, 28-29 February 2015 (Sains Malaysiana Volume 45, No. 11 (November 2016), pg. 1675–1678).
 - 6 Muhammad Luqman Mohd Napi, Nafarizal Nayan, Mohd Khairul Ahmad, **Fatin Izyani Mohd Fazli**, Noor Kamalia Abd Hamed. “Fabrication of Fluorine Doped Tin Oxide with Different Volume of Solvents on FTO Seed Layer by Hydrothermal Method” Proceeding of Conference on Nano-& Biosource Technology 2015 (NBT 2015), UKM Bangi, Selangor, 28-29 February 2015 (Sains Malaysiana Volume 45, No. 8 (August 2016), pg. 1207 – 1211).
 - 7 Noor Sakinah Khalid, Indah Fitriani Hamid, Noor Kamalia Abd Hamed, **Fatin Izyani Mohd Fazli**, Soon Chin Fhong, Mohd Khairul Ahmad. “Application of TiO₂ Nanostructure Using Hydrothermal Method For Waste Water Treatment.” Proceeding of International Conference on Electrical and Electronic Engineering 2015 (IC3E2015), Equatorial Hotel, Melaka, 10-11 August 2015 (pending publication in ARPN Journal of Engineering and Applied Sciences with Scopus indexed).
 - 8 Muhammad Luqman Mohd Napi, M.F. Maarof, Soon Chin Fhong, Nafarizal Nayan, **Fatin Izyani Mohd Fazli**, Noor Kamalia Abd Hamed, Salina Mohamad Mokhtar, Ng Kim Seng, Mohd Khairul Ahmad, Suriani Abu Bakar, Azmi Mohamed. “Fabrication of Fluorine Doped Tin Oxide (FTO) Thin Films Using Spray Pyrolysis Deposition Method for Transparent Conducting Oxide” Proceeding of Malaysian Technical Universities Conference on Engineering and Technology 2015, KSL Resort Hotel, Johor Bharu, 11 October-13 October 2015, ARPN Journal of Engineering and Applied Sciences (JEAS).
 - 9 Salina Mohamad Mokhtar, Mohd Khairul Ahmad, N.M.A.N. Ismail, Mohamad Hafiz Mamat, **Fatin Izyani Mohd Fazli**, Noor Kamalia Abd

Hamed, Muhammad Luqman Mohd Napi, Noor Sakinah Khalid, Ng Kim Seng, Nurfarina Zainal, Soon Chin Fhong, Suriani Abu Bakar, A. Muhammad. "Fabrication of Co/SnO₂ on Glass Substrate Using Spray Pyrolysis Deposition Technique with Variation of Annealing Temperature" Proceeding of Malaysian Technical Universities Conference on Engineering and Technology 2015, KSL Resort Hotel, Johor Bharu, 11 October-13 October 2015, ARPN Journal of Engineering and Applied Sciences (JEAS).

- 10** Muhammad Luqman Mohamad Napi, **Fatin Izyani Mohamad Fazli**, Soon Chin Fhong, Nafarizal Nayan, Suriani Abu Bakar, Azmi Mohamed, Mohamad Hafiz Mamat, Masaru Shimomura, Kenji Murakami. "A facile method for nanorice/nanospherical fluorine doped tin oxide using hydrothermal method for Dye-sensitized solar cell application" *Ceramics International*. (In review)

CHAPTER 1

INTRODUCTION

This chapter introduces the Dye-Sensitized Solar Cell (DSSC) and the history of its findings. Recent advances are also mentioned and continued in chapter 2. The problem statement, objectives and scopes of this study is stated in this chapter.

1.1. Solar cell technology

Solar cells are also known as a type of photovoltaic device which basically converts light or photon energy to electrical currents. The concept of the working principle of solar cells is similar as photosynthesis in plants [1]. Solar cells are considered as an attractive alternative for an energy source for its minimal impact on environment and sustainability [2].

There are three generations or categories of solar cells as summarized in Figure 1.1. The first generation is the silicon solar cells. The first generation of solar cells is defined by their silicon wafer base. This generation of solar cell is the most commonly used on building rooftops despite the high manufacturing cost that came with the use of silicon wafers. Even when the materials used are expensive, this type of solar cell generates the highest conversion efficiency with the average of 15-25 % [3][4]. This generation of solar cell also has high stability [5].

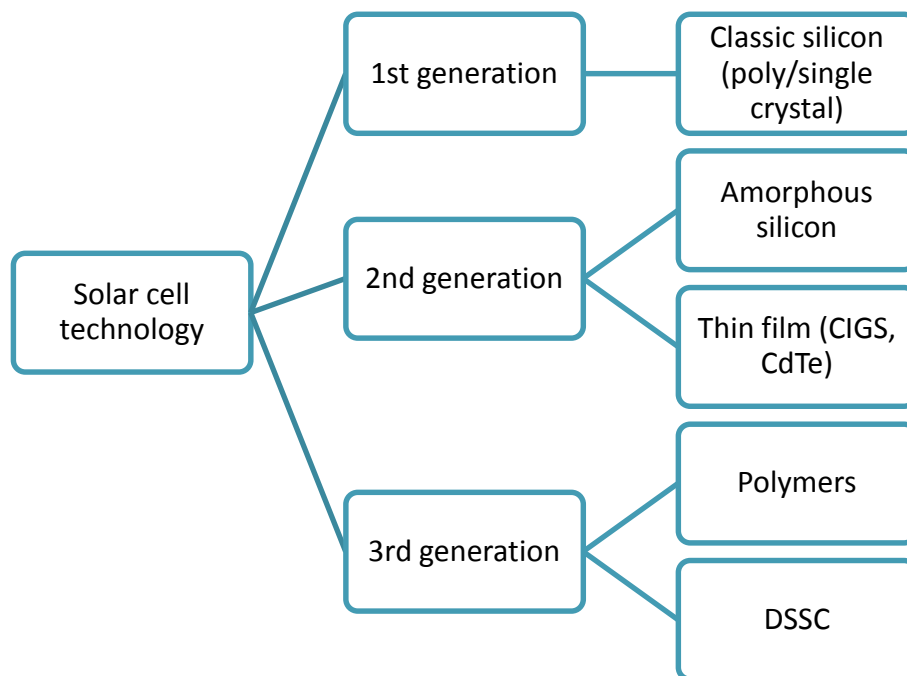


Figure 1.1: Generations of solar cell technology.

The second generation of solar cell features thin film solar cells made with amorphous silicon, copper indium gallium selenide (CIGS) and cadmium telluride (CdTe) which can be made to be far more flexible than the first generation with significantly lower cost for materials used; though the manufacturing of this type of solar cells still require high temperature treatment and vacuum processes, which are energy consuming [6–8].

The third generation of solar cells are not as commercially available as the first and second generation of solar cells and are mainly still in the process of improvements under laboratory conditions. Dye sensitized solar cells (DSSCs) are an example from this generation. The main objective of this generation is to provide a lower cost of solar cells that are also efficient over a wider band of photon energy [9, 10]. Third generation solar cells feature a lot of materials other than silicon with a variety of different structures other than using more conventional fabricating methods in order to complete its objective [11, 12].

1.2. Background of study

The nonrenewable energy sources are rapidly diminishing, thus leading to studies on renewable energy around the world. Solar cells come as the leading choice for this purpose. A great alternative choice for the current solar cell would be the dye-sensitized solar cell (DSSC) for it is effective in both cost and conversion efficiency. In 1839, the photovoltaic (PV) effect was discovered by a French physicist, Alexandre-Edmond Becquerel which opened the door to solar cell technology. Becquerel's experiment was conducted by illuminating two electrodes coated by light sensitive materials, AgCl or AgBr, using different types of light. The electricity was found increased as the light intensity increased. Charles Fritts constructed what was probably the first true solar cell in 1894. He coated selenium which is a semiconductor material with a very thin layer of gold. The efficiency of the device was only about 1% and couldn't be used as an energy supply, but were later used as light sensors. In 1954, three researchers, Gerald Pearson, Daryl Chapin and Calvin Fuller [13] of Bell Laboratories discovered the silicon solar cell, which was the first material to directly convert enough sunlight into electricity to run electrical devices. The efficiency of the silicon solar cell was 4%, which later increased to 11%. The cells were made by hand and cost \$1000 per watt. Nowadays, the silicon solar cells are known to yield an efficiency of more than 40% [14], which is remarkable considering its inexhaustible source. The theory of using illuminated dye molecules to generate electricity was further employed in a research conducted by Gerischer [15] as an effort in lowering the cost of photovoltaic devices. Further researches were done on how to improve the efficiency and stability of the DSSC. In 1991, modern type DSSC was co-invented by Michael Grätzel and Brian O'Regan [16] at UC Berkeley and was also called Grätzel cell with the efficiency of 7.1% to 7.9%.

A part that contributes to the general function of a DSSC is a metal oxide semiconductor thin film that acts as a charge collector and a base for sensitizer molecules to be adsorbed onto. The most commonly employed oxide for the purpose of DSSC is TiO₂, other than ZnO, Cu₂O, SnO₂ and Nb₂O₅ for their stability due to their wide band gap and also for their photocatalytic properties. Other than photovoltaic

devices, TiO_2 is also known to have a role in gas sensors [17], display devices [18], photo-induced water splitting [19], waste water treatment [20] and even in paint [21].

Many researches have been done to improve the efficiency and overall stability of DSSC [22]. The most advanced and recent DSSC is achieved with the highest conversion efficiency of 13% [23]. This is a very huge finding in the history of DSSC. This high efficiency is caused by an efficient semiconductor thin film; the dye and electrolyte used also plays a large part in increasing the electron mobility and the current flow [24, 25].

Some of the properties of TiO_2 can be improved as to boost the efficiency of the DSSC. For example, an increment of the surface area of TiO_2 thin film will allow for more dye molecules to be adsorbed, thus adding to the number of electron released from the dye under illumination [26]. One can increase the surface area of the thin film by constructing the TiO_2 molecules in the form of nanoflowers [27], nanorods [28], nanotubes [29] or nanowires [30]. Another means to increase the surface area is to increase the porosity of the thin film as to be done in this study.

1.3. Problem statement

Photoelectrons must travel a distance before reaching the transparent conducting oxide (TCO) layer. If the distance is too long, the photoelectrons can lose energy and fall back to ground state. It is important that the TiO₂ layer is not too thick that the photoelectrons will recombine. On the other hand, if the TiO₂ layer is too thin, there may not be enough TiO₂ particles for the dye to attach onto which will result in lower dye adsorption. Low dye adsorption will then result in lower current density due to lower amount of photoelectrons. The main focus in attempts on improving the TiO₂ thin film is to increase dye adsorption and electron mobility. Annealing of TiO₂ samples can produce a more pure sample with better crystallinity and electron mobility but high temperatures can also result in the necking of particles which will reduce surface area for dye adsorption. The TiO₂ thin film used should have an optimum thickness and annealed at an optimum temperature to achieve the highest efficiency.

1.4. Hypothesis

Increasing the thickness of photoanode might lower the transmittance of the film, thus reducing incident light to be absorbed by the dye molecules [31]. Thick TiO₂ film will also increase the chances of recombination of the photoelectrons [32]. The efficiency of a DSSC strongly depends on the surface morphology and electronic properties of the photoanode with thickness ranging from a few hundred nanometers up to 20 μm [33]. Annealing process can eliminate excessive solvent and impurities which can increase electrically-connected link of TiO₂ particles and affect the thickness of the film [34]. Annealing can improve porosity of a film but high temperatures can also result in necking of the particles [35]. Porosity of a film is associated with annealing temperature and time duration, which will affect the amount of dye adsorbed and photocurrent density [36]. Rutile on its own have poor photocatalytic activity and is prone to recombination while anatase is far superior in the application of DSSC. However, a synergistic effect between anatase and rutile exists in mixed-phase TiO₂ nanocomposites such as P25 that is supposed to enhance the photocatalytic activity of anatase [37–39].

1.5. Objectives

The objectives of this study were as follows:

- i. To investigate the surface morphology, structural property and efficiency of TiO₂ thin films in a DSSC fabricated by spray pyrolysis deposition (SPD) method.
- ii. To obtain the optimum thickness of the TiO₂ thin film for the best optical transmittance by varying the amount of TKC-303 (TiO₂ colloid) solution.
- iii. To increase the current density of fabricated DSSC by providing larger surface area for dye adsorption on the TiO₂ thin films through annealing at different temperatures and annealing time duration.

1.6. Project scopes

The project were conducted in accordance to the following scopes:

- i. Deposition of TiO₂ thin films by spray pyrolysis deposition method using a regular airbrush.
- ii. Volume of TKC-303 solution is varied to be 5 ml, 10 ml, 15 ml and 20 ml.
- iii. Annealing temperature is varied at 300 °C, 400 °C and 500 °C.
- iv. Annealing time duration is varied for 1 hour, 3 hours, 10 hours and 24 hours.
- v. Measurement of thickness by using a surface profiler.
- vi. Observations of the surface morphology of thin films using FESEM.
- vii. Analysis on the crystal state and crystal structure by an XRD machine.
- viii. Testing of DSSC efficiency by using the Solar Simulator.
- ix. Optical properties analysis by UV-Vis Spectrophotometer.

CHAPTER 2

LITERATURE REVIEW

This section discussed further about the DSSC and its components; the TiO₂ film, dye sensitizers, electrolyte and counter electrode. The SPD method is also discussed including previous researches using the same method. The methods of characterization were also mentioned in this chapter.

2.1. Dye sensitized solar cell (DSSC)

Solar cell with the highest conversion-efficiency would be a multi-junction solar cell at more than 41 % [40] and there is still a new multi-junction solar cell said to be able to exceed this limit. For a DSSC, the conversion-efficiency is not as high as other types of solar cells used nowadays with 13 % efficiency being the highest. But the fact that DSSCs use low cost materials with some of it can be readily found in nature and also low production cost has put DSSC under attention in the photovoltaic (PV) field.

DSSC differs from the conventional solar cells because it only uses one type of semiconductor as can be seen in Figure 2.1, only for the purpose as a charge carrier transport, while p-n junction solar cells uses two types of semiconductors for light absorption and charge carrier transport. However, until now their overall efficiency has been lower than silicon-based solar cells, mostly because of the innate voltage loss during the regeneration of the sensitizing dye [32, 33].

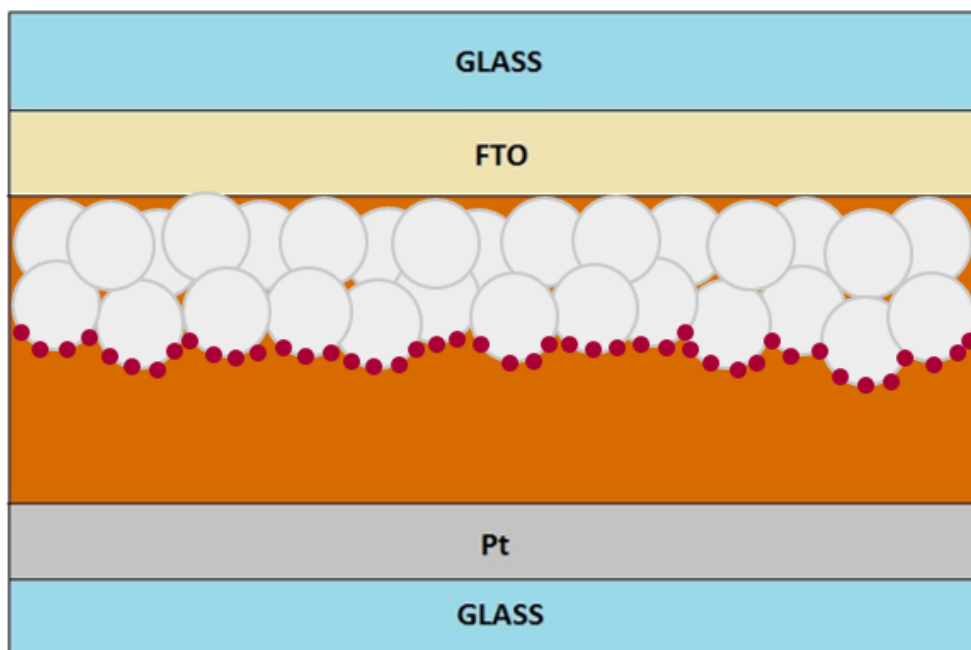
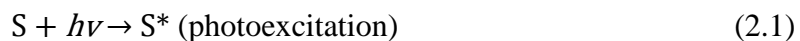


Figure 2.1: Layers of DSSC components.

The basic operational principle of a DSSC mimics the first stage of photosynthesis in that they both use sunlight to convert the energy into chemical energy which is then applied to something else. For DSSC, the photo-induced electrons flow and generate current throughout the circuit. Figure 2.2 simplifies the working process of a DSSC. The process starts when the photoanode absorbs an incident solar energy ($h\nu$). Photo-excitation of the dye molecules, S will occur and the excited electrons will be injected into the conduction band of the mesoporous semiconductor material. The process is as shown below:



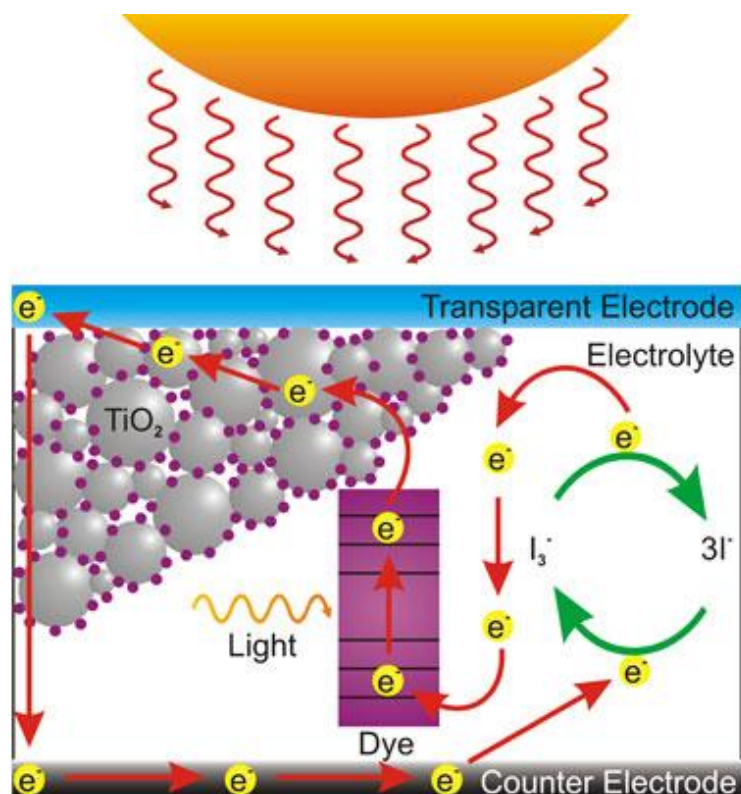


Figure 2.2: A schematic diagram of a DSSC showing the principles of operation [43].

The electrons will flow through the mesoporous TiO_2 , to the collector electrode which is the transparent conductive oxide, before travelling to the external circuit through a load in a form of a current. When the electrons reach the counter electrode/ cathode, redox triiodide electrolyte ($3\text{I}^-/\text{I}_3^-$), which is in contact with both the electrodes, will oxidize at the anode as they donate electrons to the oxidized dye molecules thus reducing it back to its ground state:



For the preparation of a DSSC, the anode component is deposited with a several micron thickness of mesoporous TiO_2 thin film. The particle size can influence the effective surface area for dye adsorption, porosity and also the pore volume for redox electrolytes to seep into the film [44]. The thin film can be really translucent or opaque depending on the method and materials of preparation [45]. The thin film will act as a base for the adsorption of the dye molecule. Dye will be adsorbed onto the TiO_2 thin film by immersing the thin film into the dye solution for

an amount of time ranging from less than an hour to overnight [46]. The DSSC is made by sandwiching the anode and cathode which is layered with a reflective, electrocatalytic thin film with a few drops of redox electrolyte in between the electrodes.

2.2. Transparent conducting oxide (TCO)

TCOs are electrically conductive oxide material with low level of light absorption. For the application of DSSC, it is almost compulsory for the TCO to be almost fully transmitting solar radiation with transmittance above 80 % in the visible to IR region. The TCO is also required to have low sheet resistance (5-15 Ω /square), and unaffected by the high temperatures of 400-500°C typically used to anneal TiO₂ samples [47]. TCO in DSSCs acts as a current collector of the photoelectrons channeled from the TiO₂. Thus it is important for the TCO used to have excellent conductivity to minimize the series resistance in the circuit for better conversion efficiency.

Other than oxides such as Zinc Oxide (ZnO) and Tin Oxide (SnO₂), conductive polymers and metal grids and films also had been attempted to be used in DSSCs [39-41]. While polymers are easy to fabricate and is flexible, and suitable metals that can be used is relatively abundant, these two materials have their own disadvantage as polymers are known to have lower electrical conductivity and transmittance, while metal conducting films can be expensive and reactive towards electrolytes used in DSSCs.

SnO₂ is an n-type semiconductor often used in DSSCs for its wide band gap (3.87 – 4.3 eV), transparency, good electron mobility and high donor concentration for dopants. Indium-doped Tin Oxide (ITO) is one of the most commonly used TCO in the applications of solar cells [51]. Even though ITO is outstanding in terms of electrical conductivity and charge transfer, its drawback lies in its high cost and limited resource other than expensive and tedious fabrication process. Therefore, as a cheaper alternative but with a comparable efficiency, FTO is commonly used as current collectors in DSSCs. SnO₂ can also be doped with other materials such as antimony and aluminum. However, using fluorine as dopant is superior in terms of transparency in the visible light region and thermal stability.

2.3. Dye sensitizers

On the mesoporous semiconductor oxide layer, photosensitizers are adsorbed to be illuminated by solar energy and excite electrons. Ever since the introduction of DSSCs, thousands of different sizes and different compounds of molecules have been tested as potential dyes. A few of desirable properties of dyes include strong light absorption in the visible and near IR region for efficient light harvesting, good solubility in organic solvents for easier deposition from stock solution onto oxide layer, possesses suitable peripheral anchoring ligands such as $-\text{COOH}$ to attach more effectively onto the oxide surface, having efficient electron injection into the conduction band of oxide layer, good thermal and chemical stability for the repetitive redox reactions. An ideal sensitizer for a PV cell converting standard air mass (AM) 1.5 sunlight into an electricity must absorb all light photons below a threshold wavelength of about 900 nm, which is equivalent to a semiconductor with a bandgap of 1.4 eV [52]. Basically, the dyes can be organic (e.g. porphyrins, phthalocyanines) or inorganic (e.g. ruthenium complex) [53].

2.3.1. Synthetic dyes

The finest PV performance in terms of both conversion efficiency and long term stability has so far been achieved by the Grätzel group with polypyridine complexes of Ruthenium (Ru); N3, N719 and 'black' dyes [54] as shown in Figure 2.3. Other than superior light harvesting properties and durability, a significant advantage of these dyes is the effective metal-ligand charge transfer transition through which the photoelectron is injected into TiO_2 . In 1993, Seigo Ito [55] published DSSCs with 10.3 % conversion efficiency using a ruthenium dye sensitizer (N3, [cis-di(thiocyanato)bis(2,2-bipyridine-4,4-dicarboxylate)ruthenium]). In Ru complexes, this metal-ligand transfer takes place at a much faster rate than the back reaction in which the photoelectron recombines with the oxidized dye molecule rather than flowing through the circuit.

Since the achievement of the 10.3 % conversion efficiency using the N3 dye, it had been difficult for researchers to reproduce the efficiency. In 2001, Nazeeruddin [56] reported DSSCs with 10.4 % efficiency by using a ruthenium dye called 'black'

dye. Even when the black dye looks green in solvent, after it has been adsorbed on a porous nanocrystalline TiO_2 electrode, the DSSC looks black due to the wide absorption band of the dye which covers the entire wavelengths in the visible range. Subsequently, Wang [57] reported 10.5 % efficiency, and Chiba [58] reported 11.1 % efficiency, when using black dye. In 2005, Nazeeruddin [59] reported a new dye which was similar to N3, N179, but achieved 11.2 % conversion efficiency in DSSC. One of the differences between the two dyes is that N3 has four H^+ counterions whereas N719 has two TBA^+ and two H^+ counterions. The difference in the counterions influences the speed of adsorption onto the TiO_2 electrode; N3 is faster (optimum adsorption time: 3h) whereas N719 is slower (optimum adsorption time: 24h).

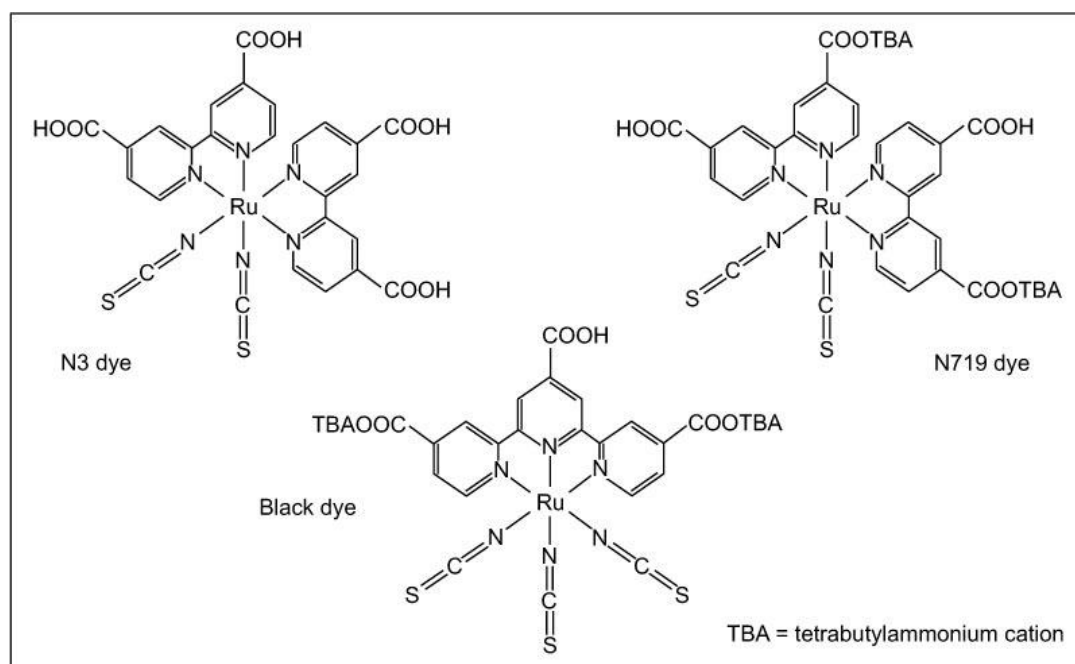


Figure 2.3: Structures of the ruthenium-based dyes N3, N719 and ‘black’ dye developed by the Grätzel group [54].

2.3.2. Organic dyes

Since the idea of DSSC came from the process of photosynthesis, a lot of natural dyes have also been studied along the effort to improve the efficiency of a DSSC. Natural dyes come in different colors, depending on the pigments and their pH value. Their performance in a DSSC also differs under the influence of a number of parameters. Contrary to the Ru-based dyes, natural dyes are far more inexpensive and abundant. Furthermore, since they are from natural occurring plants, they are also significantly less hazardous to the environment with easier disposal. Even so, dyes extracted from natural occurring plants does not produce efficiencies as high as that of the synthetic dyes [52].

The flavonoids are an extensive group of natural products that include a C₆–C₃–C₆ carbon basis or more specifically, a phenylbenzopyran functionality. The anthocyanins is a major part of the flavonoid group that is responsible for cyanic colors ranging from salmon pink to red, and violet to dark blue of a lot of flowers, fruits and leaves. They can also exist in other plant tissues; for example, roots, tubers and stems [60]. The most common anthocyanidins found in flowers are pelargonidin (orange), cyanidin (orange-red), petunidin (blue-red) and malvidin (blue-red) with their structures shown in Figure 2.4 [61]. They are the most abundant and widespread of the flavonoid pigments that absorb light at the longest wavelength. Anthocyanins are found in cell vacuole located in flowers and fruits; although they may also be located in leaves, stems and roots in the outer parts such as the epidermis and peripheral mesophyll cells.

The highest conversion efficiency of 2.63 % by using natural dye was reported by Maiaugree [62]. The research also reported the use of natural counter electrode on poly (3,4-ethylenedioxythiophene) polystyrene sulfonate (PEDOT-PSS). Both the dye and the carbon material were derived from mangosteen peel waste. Another example of the use of natural dye with significant conversion efficiency was reported by Calogero [63]. The dye used was extracted from a red turnip. The conversion efficiency obtained was 1.7 % under AM 1.5 irradiation. The report also mentioned the use of purple extract from the wild Sicilian prickly pear fruit which obtained 1.26 % conversion efficiency.

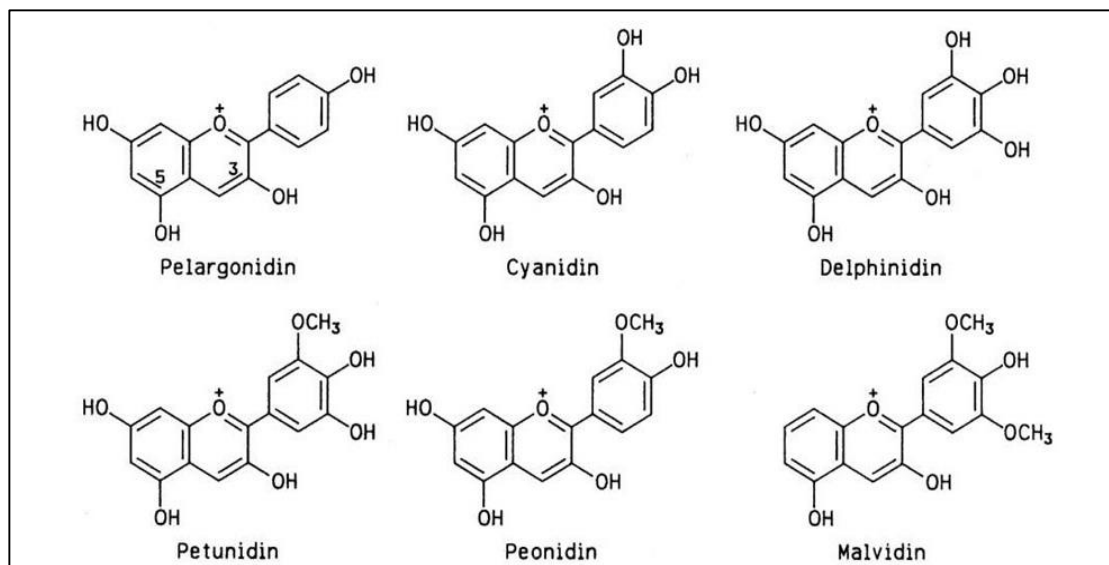


Figure 2.4: Structures of common anthocyanidins found in natural foods [61].

2.4. Electrolytes

The role of an electrolyte is to facilitate the transport of the electron between the working electrode and the counter electrode. Electrolytes for DSSC can be classified into 3 types; solid, liquid and quasi-solid as shown in Figure 2.5. A few ideal properties of an electrolyte include low viscosity to ease electron diffusion, good interfacial contact with the working and counter electrode, low vapor pressure to ensure long term stability of the DSSC, high boiling point, and high dielectric properties. Other important qualities include chemical inertness, environmental sustainability and simple fabrication process.

A lot of redox electrolyte have been tested in the effort to find the best electrolyte for DSSCs. The most favorable electrolyte found was the triiodide/iodide couple. Various solvents have also been tested to achieve an electrolyte with the best performance even under extreme conditions. For example, acetonitrile as solvent can provide low viscosity for the electrolyte, but has low boiling point and high vapor pressure; making it unable to withstand temperatures higher than 80°C.

The electrolyte used in this research is a type of liquid electrolyte. Liquid electrolytes uses liquid solvents as a medium for the redox couple of the electrolyte. Liquid electrolytes can be roughly divided into two; organic solvents as used in this research, and ionic liquid electrolytes. One of the most common organic solvents

used is acetonitrile based on its efficiency as have been proven by Grätzel & O'Regan [16], by mixing it with ethylene carbonate. While acetonitrile has low viscosity and good solubility as it can dissolve a wide range of organic compounds and salts, it is also volatile with high vapor pressure. Other nitriles such as glutaronitrile, valeronitrile and propionitrile have also been studied alongside with other organic solvents from alcohols to water. Two types of nitriles, 3-methoxypropionitrile and butyronitrile were found to be less volatile than acetonitrile, while also has higher boiling point and good performance stability. The downside to these nitriles is that they have higher viscosity than acetonitrile and as a result, it exhibits lower efficiencies.

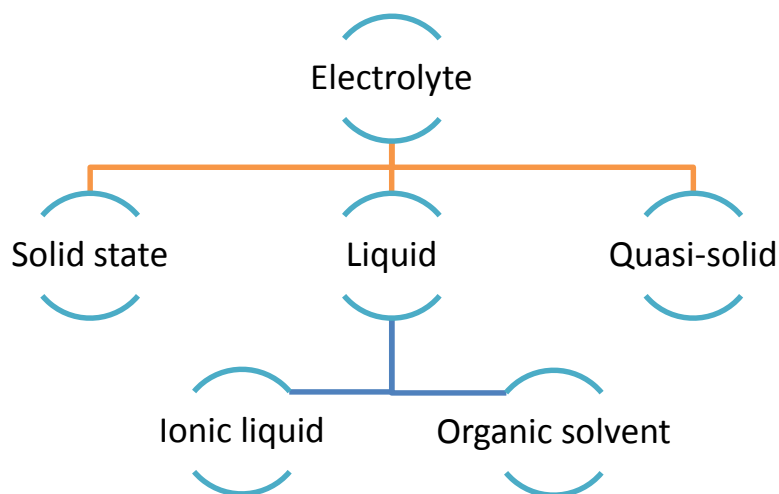


Figure 2.5: Classification of electrolytes for DSSC [24].

2.5. Counter electrode

The counter electrode also known as cathode functions to reduce the oxidized form of the electrolyte as it provides electrons flowing from the outer circuit. The cathode component is usually lined with Pt for its good electrocatalytic properties, high exchange current density and reflectivity. Though Pt is a rare and expensive substance, only a small amount is needed to make a highly effective cathode [64]. Pt

also acts as a catalyst to accelerate the reduction reaction of the electrolyte. But due to the high cost of Pt, other substances like graphene and conductive polymers are also being used as alternative materials for the counter electrode [65].

2.6. Titanium dioxide nanostructures

Titanium dioxide (TiO_2), also known as titania, exists in nature as an oxide of titanium and is relatively abundant. It exists in a lot of different forms with the three most accessible forms being rutile (tetragonal), anatase (tetragonal) and brookite (orthorhombic). The basic structure of the three TiO_2 forms are as shown in Figure 2.6. Rutile is the more thermodynamically stable form of TiO_2 if compared to anatase [66], though the fact is only for macroscopic crystals. For nanocrystals with sizes of about 10-20 nm, anatase is the more stable form which regarding on their sizes, in agreement with a research conducted to compare diamonds and graphite [67]. Rutile can be produced synthetically by annealing anatase at the temperature of 700-1000 °C since anatase is metastable [68]. Researches on brookite is not as much as the ones on anatase and rutile because it is rare in nature and the synthesis of pure brookite is difficult [69].

In the application of DSSC, anatase is a much more popular selection as a photoanode due to high electron mobility and superior photocatalytic activities [70]. Since the anatase conduction band is more negative by 0.2 V than rutile, a higher maximum photovoltage can be achieved by using anatase photoanode than rutile if the same redox mediator is used [71]. However, there is also a theory that by mixing anatase and rutile which has lower energy, the transfer of electrons from anatase rutile electron trapping site helps to lessen the rate of recombination for anatase, leading to more effective electron-hole separation and improved catalytic reactivity [72]. However, the data used to support this theory is inconclusive and need further research since there can be a lot of factors that can influence the synergistic effect between anatase and rutile.

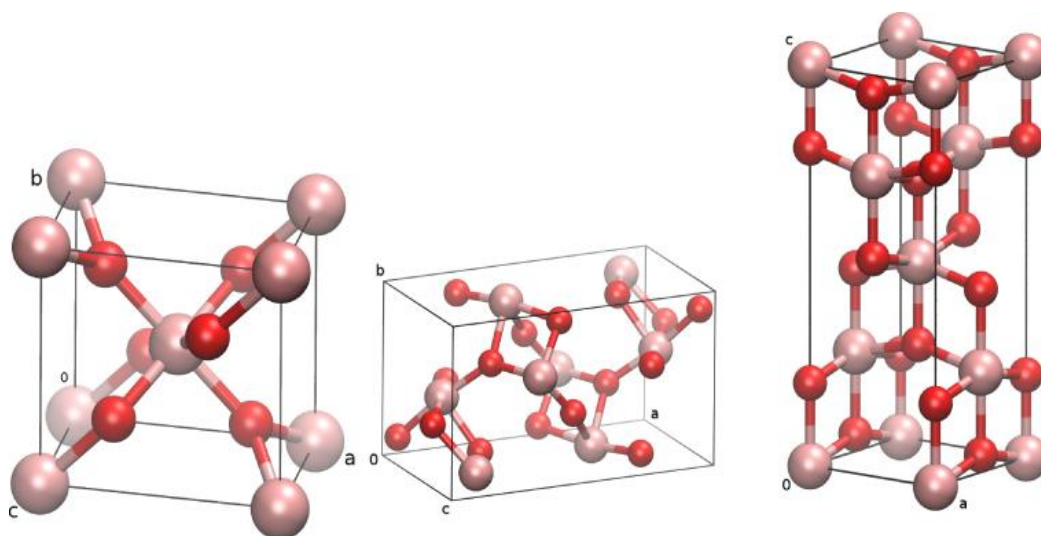


Figure 2.6: Unit cells of the TiO_2 modifications rutile, brookite and anatase (from left to right) [73].

TiO_2 is used as a layer of electron acceptors for DSSC for its wide band gap and thus, stability. The band gaps for rutile and anatase are 3eV and 3.2eV respectively. The band gaps for both materials are indirect. Though there are other oxide semiconductors that fit the role as well, TiO_2 turns out to be the most versatile for allowing the DSSC to have the highest solar conversion efficiency. TiO_2 is also very inert and non-reactive, non-toxic and readily available in huge quantities. One of the applications of TiO_2 is as pigments in white paints, for its brightness and very high refractive index [74]. This property of TiO_2 is also of use for other researches for example, in antireflective coatings [75]. Thousands of publications have written on the preparation of colloidal particles of TiO_2 by the solvothermal reactions based on titanium n-butoxide and acetic acid which can yield TiO_2 of many morphologies from nanoparticles [76], nanowires [77], nanofibers [78], nanosheets [79] and nanotubes [80].

TiO_2 naturally has high transport mobility of the charge carrier that reduces the electron-transport resistance but its performance can be improved. Synthetic or naturally occurring TiO_2 are both slightly oxygen deficient, TiO_{2-x} ($x \approx 0.01$). This small deficiency makes room for n-type doping which can reduce its band gap and increase its photocatalytic properties [81]. Double layer structured TiO_2 can increase the transport mobility of the TiO_2 film [82]. It is done by depositing an underlayer of large size particles (200-300 nm) before a layer of nanoparticles (10-30 nm) on top.

This creates a larger surface area and better transport mobility at the same time. A loss path in DSSC is the recombination of the injected electrons with the electrolyte. The result of this phenomenon is the dark current, which diminishes the efficiency of a DSSC. This situation can be prevented and minimized by modifying the structure of TiO_2 . This modification can be employed by adding insulating or blocking layer, and by treating the surface of the TiO_2 . The treatments can be classified into mechanical or chemical method.

Chemical vapor deposition, chemical and electrochemical treatment, sol-gel and biochemical are examples of chemical treatment method. This method involves chemical reactions at the interface between the material and chemical used. Mechanical treatment method includes etching, blasting, polishing, shaping and other physical treatments. The main goal of this method is to obtain certain roughness and topography aside from removing surface contaminants and improving adhesion quality if necessary [83].

Annealing of TiO_2 thin films, which can be included as one of the mechanical treatments, can improve their surface morphology and crystallinity which can heavily influence the electron transport rate and effective surface area [84]. Annealing process evaporates the solvent used in the preparation of the thin film, resulting in purer and more crystalline structure. The annealing process may affect the thickness of the film but not necessarily as reported in a previous research [85]. Instead of thinning the film, annealing process changes the structure of the film from amorphous to a more porous and crystalline structure. It was also reported that annealing of the films makes the grain size becomes larger, lowers the transmittance of the film, increase the value of refractive index and allowed indirect optical band gap [43]. Other than that, annealing process was also reported to make the surface rougher as the temperature increase [86].

Annealing under the influence of oxygen and nitrogen gas can improve the structure of the TiO_2 thin films fabricated even more than annealing in air. Annealing under the influence of nitrogen gas can add ligands on the surface of the TiO_2 particles so that the dye molecules can attach better on the surface. This kind of annealing gives an extra advantage on films for DSSC application. Annealing of TiO_2 in oxygen gas is much like doping in oxygen into the TiO_2 structure. It can increase the electron mobility of the TiO_2 films.

2.7. Fabrication method

TiO₂ thin film for DSSC can be fabricated to be in various shapes and sizes depending on the methods and materials used as summarized in Figure 2.7. TiO₂ can be produced by using hydrothermal method [87], sputtering method [88], chemical vapor deposition [89], doctor blading [90], pulsed laser deposition [91] and spray pyrolysis deposition method [92], to name a few.

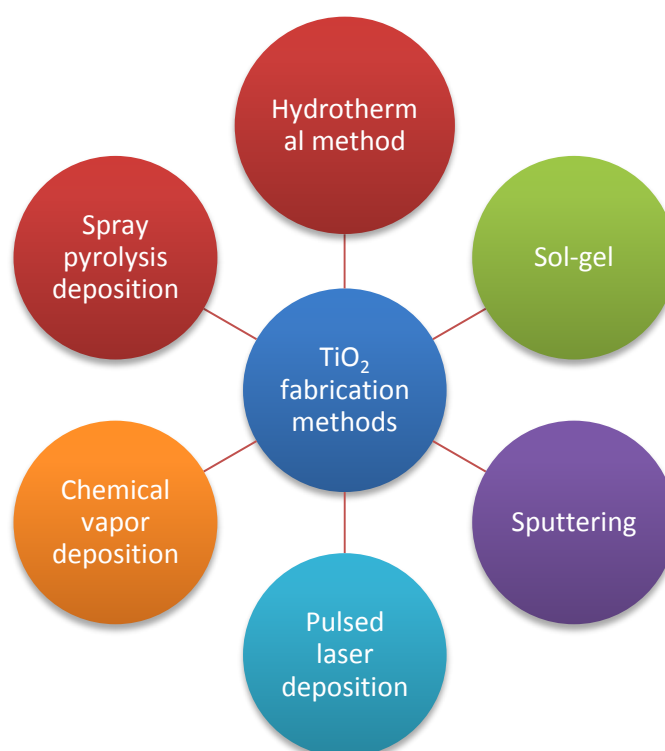


Figure 2.7: TiO₂ fabrication methods.

Hydrothermal method is a method of crystallizing substances using a solution heated in a closed system under a controlled pressure. The closed system frequently used in previous researches is an autoclave. The pH of the solution, the temperature and the pressure applied on the system can determine the shape of the crystals and the phase; whether it is rutile or anatase. It was also reported that the formation of pure brookite crystals is also possible by hydrothermal method [93].

Sputtering method is when atoms are ejected from a target bombarded by an accelerated particle onto a substrate to create a thin film. The thickness of the thin

film is varied by the sputtering deposition time. Sputtering method is an effective method to create Pt thin film for the counter electrode as it can create a minimum thickness for a highly efficient counter electrode. Pulsed laser deposition method is quite similar to the sputtering method except that it uses a pulsing laser to bombard the target and not an energetic particle.

Chemical vapor deposition (CVD) is a chemical process used to produce high quality and high-performance thin film. The substrate is exposed to one or more volatile precursors, which react and decompose on the substrate surface to produce the desired deposit. Frequently, volatile by-products are also produced, which are removed by gas flow through the reaction chamber. Doctor blading or blade coating is a method practiced in the making of thin film on a large surface area rigid or flexible substrate. The thickness of the film is determined by the distance of the blade to the substrate surface. It is a simple yet effective method of thin film deposition.

Spray pyrolysis deposition (SPD) is a liquid phase chemical deposition method of a thin film involves the spraying of a solution onto substrates placed over a heated surface where the solvent will evaporate to form a solid chemical compound. The compound used to produce a thin film by this method should be volatile at the temperature of deposition. SPD technique is one of the easiest and cost-effective methods in the preparing thin films of different thickness, ceramic coatings and powders. This method is suitable for a wide range of compositions and often does not require special types of substrates. This method can also be employed in the making of dense or porous films [81, 82], multi-layered films [96] and also powder production [97].

2.7.1. Spray pyrolysis deposition (SPD) method

The schematic representation of SPD apparatus is shown in Figure 2.8. Typical SPD equipment consists of an atomizer, a heater with a temperature controller, and a solution that will come out of a nozzle. There are a few types of atomizer for SPD technique; air blast or air compressor where the solution is exposed to a stream of air, ultrasonic that produces short wavelengths for fine atomization and electrostatic where the solution is exposed to high electric field. The substrate surface temperature is important in determining the surface morphology of the resulting thin film. Higher

temperature can change the surface from dense to slightly cracked and then to a porous structure. The surface structure of the film can influence its optical and electrical properties [92].

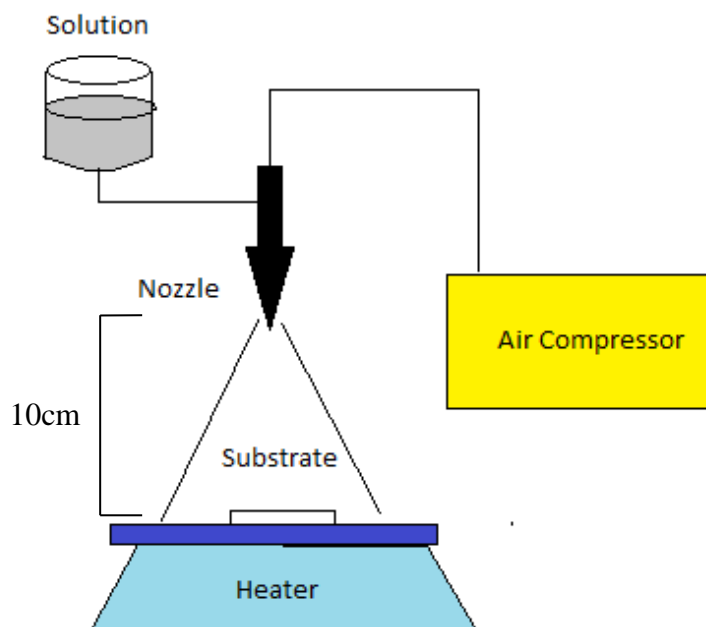


Figure 2.8: An illustration of spray pyrolysis deposition technique.

An example of TiO_2 by SPD method was performed by Masayuki Okuya [98]. The source solution of titanium (IV) oxy acetylacetonate 2-butanol was atomized by a nozzle with 3.0 kg/cm^2 of compressed air. The mist was transported onto a heated glass substrate (Corning 1737, 25mm x 25mm x 1mm in size) with the distance between the nozzle and the glass substrate about 300 mm. The parameter of this experiment is the substrate surface temperature which varied from 300 to 500 °C. The film formation was carried out intermittently since the mist will cool down the substrate temperature. When the substrate temperature was recovered, the process was resumed. The spray rate of the solution and the period for each spraying was fixed at 1.0 ml/s and 0.5 s respectively. The results of this research showed that the samples obtained are anatase, though the samples deposited on substrate with surface temperature of 300 °C are amorphous. The optimum surface temperature to grow anatase by SPD method according to this research was 350 °C.

According to a paper discussing the SPD method by Perednis and Gauckler [92], this method involves processes that occur either sequentially or simultaneously. A few of the main processes involved aerosol generation and transport, droplet impact and spreading, solvent evaporation and precursor decomposition. They also stated that the temperature of the substrate will determine the morphology and properties of the film fabricated [99]. Increasing the temperature of the substrate can change the morphology of the film from dense or cracked to a more porous structure. Figure 2.9 shows how the surface temperature will affect the precursor solution in the deposition process.

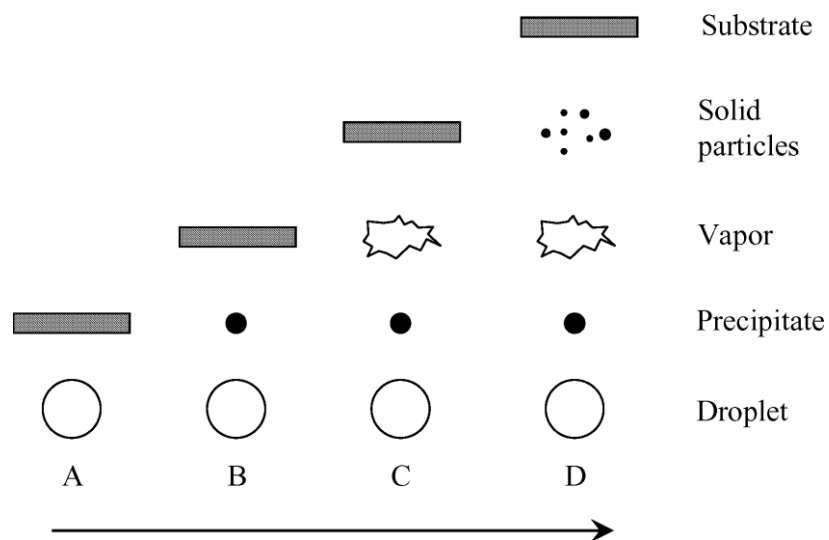


Figure 2.9: Illustration of the deposition process with increasing substrate temperature [92].

2.8. Summary

DSSC is a type of solar cell that produces a lower efficiency than a conventional solar cell but it has a few attractive advantages in terms of cost and minimal impact on the environment. TiO_2 is a type of semiconductor that is most popular to be used in a DSSC as a base for dye sensitizers and a photoanode. TiO_2 can be fabricated in many ways but the SPD method is applied in this research for its simple and low cost process next to the fact that it is versatile for the ability to deposit on a wide range of surfaces. N719 dye is a type of synthetic ruthenium dye famous for having a wide range of absorbance and thus selected and used in this research. The electrolyte used is the triiodide redox electrolyte in acetonitrile solvent for low viscosity and good solubility. Pt electrode is selected to be used for it is known to have good conductivity, highly reflective and is inert when used with the electrolyte.

CHAPTER 3

RESEARCH METHODOLOGY

The TiO₂ thin films are prepared by spray pyrolysis deposition method on fluorine-doped tin oxide (FTO). The flow chart of the methodology is as in Figure 3.1. Four sets of TiO₂ thin films were fabricated with different parameters; TKC volume, annealing temperature and time, and pure anatase TiO₂. The films are then characterized by using X-ray Diffractometer (XRD), Field Emission Scanning Electron Microscopy (FESEM) UV-Vis Spectrophotometer (UV-Vis), Surface Profiler and a Solar Simulator.

3.1. Substrate preparation

The substrate used in this study is the FTO on glass and was prepared according to the steps listed in Figure 3.2. The dimension of the substrates is 2cm x 1cm. the substrates are cleaned by an ultrasonicator in distilled water, ethanol and propanol solution of the same ratio 1:1:1. The ultrasonic cleaning is done for 10 minutes with the heat off. The cleaned substrates are then left in air to dry before masked by a piece of punctured aluminum foil as shown in Figure 3.3 with the area of the hole being 0.25 cm². The substrates are then put onto a hotplate and was heated up to 150 °C. A total of 8 substrates are used for each deposition process.

REFERENCES

- [1] I. McConnell, G. Li, and G. W. Brudvig, "Energy Conversion in Natural and Artificial Photosynthesis," *Chem. Biol.*, vol. 17, no. 5, pp. 434–447, May 2010.
- [2] L. M. Peter, "Towards sustainable photovoltaics: the search for new materials," *Philos. Trans. R. Soc. London A Math. Phys. Eng. Sci.*, vol. 369, no. 1942, 2011.
- [3] M. Green, "The path to 25% silicon solar cell efficiency: history of silicon cell evolution," *Prog. Photovoltaics Res.*, 2009.
- [4] M. Taguchi, A. Yano, and S. Tohoda, "24.7% record efficiency HIT solar cell on thin silicon wafer," *IEEE J.*, 2014.
- [5] A. Shah, H. Schade, M. Vanecek, and J. Meier, "Thin-film silicon solar cell technology," *Prog.*, 2004.
- [6] J. Yang, A. Banerjee, and S. Guha, "Triple-junction amorphous silicon alloy solar cell with 14.6% initial and 13.0% stable conversion efficiencies," *Appl. Phys. Lett.*, 1997.
- [7] T. Söderström, F.-J. F. Haug, V. Terrazzoni-Daudrix, and C. Ballif, "Optimization of amorphous silicon thin film solar cells for flexible photovoltaics," vol. 103, no. 11, p. 114509, Jun. 2008.
- [8] S. Lee, R. Biswas, W. Li, D. Kang, L. Chan, and J. Yoon, "Printable nanostructured silicon solar cells for high-performance, large-area flexible photovoltaics," *ACS Nano*, 2014.
- [9] F. Bella, N. Mobarak, F. Jumaah, and A. Ahmad, "From seaweeds to biopolymeric electrolytes for third generation solar cells: An intriguing approach," *Electrochim. Acta*, 2015.
- [10] H. Snaith, "Perovskites: the emergence of a new era for low-cost, high-efficiency solar cells," *J. Phys. Chem. Lett.*, 2013.
- [11] Z. Beiley, M. Christoforo, and P. Gratia, "Semi-Transparent Polymer Solar Cells with Excellent Sub-Bandgap Transmission for Third Generation Photovoltaics," *Advanced*, 2013.
- [12] B. He, X. Meng, Q. Tang, P. Li, S. Yuan, and P. Yang, "Low-cost CoPt alloy counter electrodes for efficient dye-sensitized solar cells," *J. Power Sources*, 2014.
- [13] D. Chapin, C. Fuller, and G. Pearson, "Solar energy converting apparatus," *US Pat. 2,780,765*, 1957.
- [14] R. King, D. Law, and K. Edmondson, "40% efficient metamorphic GaInP/GaInAs/Ge multijunction solar cells," *Appl. Phys.*, 2007.
- [15] H. Gerischer, M. Michel-Beyerle, and F. Reberstrost, "Sensitization of charge injection into semiconductors with large band gap," *Electrochimica*, 1968.
- [16] B. O'regan and M. Grfitzeli, "A low-cost, high-efficiency solar cell based on dye-sensitized," *Nature*, 1991.

- [17] G. Mor, M. Carvalho, and O. Varghese, "A room-temperature TiO₂-nanotube hydrogen sensor able to self-clean photoactively from environmental contamination," *Mater. Res.*, 2004.
- [18] K. Iuchi, Y. Ohko, T. Tatsuma, and A. Fujishima, "Cathode-separated TiO₂ photocatalysts applicable to a photochromic device responsive to backside illumination," *Chem. Mater.*, 2004.
- [19] S. Khan, M. Al-Shahry, and W. Ingler, "Efficient photochemical water splitting by a chemically modified n-TiO₂," *Science* (80-.), 2002.
- [20] X. Li and F. Li, "Study of Au/Au³⁺-TiO₂ photocatalysts toward visible photooxidation for water and wastewater treatment," *Environ. Sci. Technol.*, 2001.
- [21] E. Reck and S. Seymour, "The effect of TiO₂ pigment on the performance of paratoluene sulphonic acid catalysed paint systems," *Macromol. Symp.*, 2002.
- [22] P. Wang and S. Zakeeruddin, "Molecular- Scale Interface Engineering of TiO₂ Nanocrystals: Improve the Efficiency and Stability of Dye- Sensitized Solar Cells," *Advanced*, 2003.
- [23] S. Mathew, A. Yella, P. Gao, and R. Humphry-Baker, "Dye-sensitized solar cells with 13% efficiency achieved through the molecular engineering of porphyrin sensitizers," *Nature*, 2014.
- [24] M. Ye, X. Wen, M. Wang, J. Iocozzia, N. Zhang, and C. Lin, "Recent advances in dye-sensitized solar cells: from photoanodes, sensitizers and electrolytes to counter electrodes," *Mater. Today*, 2015.
- [25] A. Chiappone, F. Bella, J. Nair, and G. Meligrana, "Structure–Performance Correlation of Nanocellulose- Based Polymer Electrolytes for Efficient Quasi- solid DSSCs," 2014.
- [26] J. Wu, G. Chen, H. Yang, and C. Ku, "Effects of dye adsorption on the electron transport properties in ZnO-nanowire dye-sensitized solar cells," *Appl. Phys. Lett.*, 2007.
- [27] F. Xu, Y. Wu, X. Zhang, Z. Gao, and K. Jiang, "Controllable synthesis of rutile TiO₂ nanorod array, nanoflowers and microspheres directly on fluorine-doped tin oxide for dye-sensitised solar cells," *Micro Nano Lett.*, 2012.
- [28] B. Liu and E. Aydil, "Growth of oriented single-crystalline rutile TiO₂ nanorods on transparent conducting substrates for dye-sensitized solar cells," *J. Am. Chem. Soc.*, 2009.
- [29] K. Zhu, N. Neale, A. Miedaner, and A. Frank, "Enhanced charge-collection efficiencies and light scattering in dye-sensitized solar cells using oriented TiO₂ nanotubes arrays," *Nano Lett.*, 2007.
- [30] B. Tan and Y. Wu, "Dye-sensitized solar cells based on anatase TiO₂ nanoparticle/nanowire composites," *J. Phys. Chem. B*, 2006.
- [31] M. C. Kao, H. Z. Chen, S. L. Young, C. Y. Kung, and C. C. Lin, "The effects of the thickness of TiO₂ films on the performance of dye-sensitized solar cells," *Thin Solid Films*, vol. 517, no. 17, pp. 5096–5099, Jul. 2009.
- [32] V. Baglio, M. Girolamo, V. Antonucci, and A. S. Aricò, "Influence of TiO₂ Film Thickness on the Electrochemical Behaviour of Dye-Sensitized Solar Cells," vol. 6, pp. 3375–3384, 2011.
- [33] M. Grätzel, "Dye-sensitized solar cells," vol. 4, pp. 145–153, 2003.
- [34] A. F. Nogueira, C. Longo, and M. De Paoli, "Polymers in dye sensitized solar cells : overview and perspectives," vol. 248, pp. 1455–1468, 2004.
- [35] W. J. Lee, D. Y. Lee, J. S. Song, and B. K. Min, "Effect of Process Parameters on the Efficiency of Dye Sensitized Solar Cells," *Met. Mater. Int.*, vol. 11, no.

- 6, pp. 465–471, Nov. 2005.
- [36] C. R. Lee, H. S. Kim, and N. G. Park, “Dependence of porosity, charge recombination kinetics and photovoltaic performance on annealing condition of TiO₂ films,” *Front. Optoelectron. China*, vol. 4, no. 1, pp. 59–64, 2011.
- [37] G. Li, L. Chen, M. E. Graham, and K. A. Gray, “A comparison of mixed phase titania photocatalysts prepared by physical and chemical methods: The importance of the solid-solid interface,” *J. Mol. Catal. A Chem.*, vol. 275, no. 1–2, pp. 30–35, 2007.
- [38] L. Chen, M. E. Graham, G. Li, and K. A. Gray, “Fabricating highly active mixed phase TiO₂ photocatalysts by reactive DC magnetron sputter deposition,” *Thin Solid Films*, vol. 515, no. 3, pp. 1176–1181, 2006.
- [39] B. Sun and P. G. Smirniotis, “Interaction of anatase and rutile TiO₂ particles in aqueous photooxidation,” *Catal. Today*, vol. 88, no. 1–2, pp. 49–59, 2003.
- [40] W. Guter, J. Schöne, S. Philipps, and M. Steiner, “Current-matched triple-junction solar cell reaching 41.1% conversion efficiency under concentrated sunlight,” *Appl. Phys.*, 2009.
- [41] T. Kinoshita, K. Nonomura, N. Jeon, and F. Giordano, “Spectral splitting photovoltaics using perovskite and wideband dye-sensitized solar cells,” *Nature*, 2015.
- [42] V. Gondane and P. Bhargava, “Tuning flat band potential of TiO₂ using an electrolyte additive to enhance open circuit voltage and minimize current loss in dye sensitized solar cells,” *Electrochim. Acta*, 2016.
- [43] M. Hasan, A. Haseeb, and R. Saidur, “Effects of annealing treatment on optical properties of anatase TiO₂ thin films,” *Int. J.*, 2008.
- [44] M. Jeng, Y. Wung, L. Chang, and L. Chow, “Particle size effects of TiO₂ layers on the solar efficiency of dye-sensitized solar cells,” *Int. J.*, 2013.
- [45] K. Lee, R. Kirchgeorg, and P. Schmuki, “Role of transparent electrodes for high efficiency TiO₂ nanotube based dye-sensitized solar cells,” *J. Phys.*, 2014.
- [46] S. Nagai, G. Hirano, T. Bessho, and K. Satori, “Raman spectroscopic study of dye adsorption on TiO₂ electrodes of dye-sensitized solar cells,” *Vib. Spectrosc.*, 2014.
- [47] R. Otsuka, T. Endo, T. Takano, and S. Takemura, “Fluorine doped tin oxide film with high haze and transmittance prepared for dye-sensitized solar cells,” *Japanese J.*, 2015.
- [48] V. Kumar, N. Singh, V. Kumar, and L. Purohit, “Doped zinc oxide window layers for dye sensitized solar cells,” *J. Appl.*, 2013.
- [49] J. Kwon, V. Ganapathy, Y. Kim, K. Song, and H. Park, “Nanopatterned conductive polymer films as a Pt, TCO-free counter electrode for low-cost dye-sensitized solar cells,” *Nanoscale*, 2013.
- [50] H. Weerasinghe, F. Huang, and Y. Cheng, “Fabrication of flexible dye sensitized solar cells on plastic substrates,” *Nano Energy*, 2013.
- [51] E. Joanni, R. Savu, M. de S. Góes, and P. Bueno, “Dye-sensitized solar cell architecture based on indium–tin oxide nanowires coated with titanium dioxide,” *Scr. Mater.*, 2007.
- [52] M. Narayan, “Dye sensitized solar cells based on natural photosensitizers,” *Renew. Sustain. Energy Rev.*, 2012.
- [53] U. Mehmood, S. Rahman, and K. Harrabi, “Recent advances in dye sensitized solar cells,” *Adv. Mater.*, 2014.
- [54] M. Ryan, “PGM HIGHLIGHTS: Progress in Ruthenium Complexes for Dye

- Sensitized Solar Cells,” *Platin. Met. Rev.*, 2009.
- [55] S. Ito, T. Murakami, P. Comte, P. Liska, and C. Grätzel, “Fabrication of thin film dye sensitized solar cells with solar to electric power conversion efficiency over 10%,” *Thin Solid Films*, 2008.
- [56] M. Nazeeruddin, P. Pechy, and T. Renouard, “Engineering of efficient panchromatic sensitizers for nanocrystalline TiO₂-based solar cells,” *J.*, 2001.
- [57] Z. Wang, T. Yamaguchi, H. Sugihara, and H. Arakawa, “Significant efficiency improvement of the black dye-sensitized solar cell through protonation of TiO₂ films,” *Langmuir*, 2005.
- [58] Y. Chiba, A. Islam, Y. Watanabe, and R. Komiya, “Dye-sensitized solar cells with conversion efficiency of 11.1%,” *Japanese J.*, 2006.
- [59] M. Nazeeruddin, F. De Angelis, and S. Fantacci, “Combined experimental and DFT-TDDFT computational study of photoelectrochemical cell ruthenium sensitizers,” *J.*, 2005.
- [60] K. Gould and C. Lister, “Flavonoid functions in plants,” *Biochem. ...*, 2006.
- [61] J. M. R. C. Fernando and G. K. R. Senadeera, “Natural anthocyanins as photosensitizers for dye-sensitized solar devices,” *Curr. Sci.*, vol. 95, no. SEPTEMBER 2008, pp. 663–666, 2008.
- [62] W. Maiaugree, S. Lowpa, and M. Towannang, “A dye sensitized solar cell using natural counter electrode and natural dye derived from mangosteen peel waste,” *Scientific*, 2015.
- [63] G. Calogero, G. Di Marco, and S. Cazzanti, “Efficient dye-sensitized solar cells using red turnip and purple wild Sicilian prickly pear fruits,” *Int. J.*, 2010.
- [64] C. Yoon, R. Vittal, J. Lee, W. Chae, and K. Kim, “Enhanced performance of a dye-sensitized solar cell with an electrodeposited-platinum counter electrode,” *Electrochim. Acta*, 2008.
- [65] A. Hagfeldt, G. Boschloo, L. Sun, and L. Kloo, “Dye-sensitized solar cells,” *Chemical*, 2010.
- [66] A. Fahmi, C. Minot, B. Silvi, and M. Causá, “Theoretical analysis of the structures of titanium dioxide crystals,” *Phys. Rev. B*, 1993.
- [67] P. Badziag, W. Verwoerd, W. Ellis, and N. Greiner, “Nanometre-sized diamonds are more stable than graphite,” *Nature*, 1990.
- [68] X. Ding and X. Liu, “Correlation between anatase-to-rutile transformation and grain growth in nanocrystalline titania powders,” *J. Mater. Res.*, 1998.
- [69] D. Reyes-Coronado and G. Rodríguez-Gattorno, “Phase-pure TiO₂ nanoparticles: anatase, brookite and rutile,” 2008.
- [70] M. Xu *et al.*, “Photocatalytic activity of bulk TiO₂ anatase and rutile single crystals using infrared absorption spectroscopy,” *Phys. Rev. Lett.*, vol. 106, no. 13, pp. 1–4, 2011.
- [71] D. Cahen, G. Hodes, and M. Gra, “Nature of Photovoltaic Action in Dye-Sensitized Solar Cells,” pp. 2053–2059, 2000.
- [72] R. I. Bickley, T. Gonzalez-Carreno, J. S. Lees, L. Palmisano, and R. J. D. Tilley, “A structural investigation of titanium dioxide photocatalysts,” *J. Solid State Chem.*, vol. 92, no. 1, pp. 178–190, 1991.
- [73] J. Moellmann, S. Ehrlich, and R. Tonner, “A DFT-D study of structural and energetic properties of TiO₂ modifications,” *J. Phys.*, 2012.
- [74] D. Hanaor and C. Sorrell, “Review of the anatase to rutile phase transformation,” *J. Mater. Sci.*, 2011.
- [75] M. Langlet, M. Burgos, C. Coutier, and C. Jimenez, “Low temperature

- preparation of high refractive index and mechanically resistant sol-gel TiO₂ films for multilayer antireflective coating applications,” *J. sol-gel*, 2001.
- [76] S. Das, S. Kar, and S. Chaudhuri, “Optical properties of SnO₂ nanoparticles and nanorods synthesized by solvothermal process,” *J. Appl. Phys.*, 2006.
- [77] H. Wu, H. Hng, and X. Lou, “Direct synthesis of anatase TiO₂ nanowires with enhanced photocatalytic activity,” *Adv. Mater.*, 2012.
- [78] R. Xie and J. Shang, “Morphological control in solvothermal synthesis of titanium oxide,” *J. Mater. Sci.*, 2007.
- [79] H. Yang, G. Liu, S. Qiao, C. Sun, and Y. Jin, “Solvothermal synthesis and photoreactivity of anatase TiO₂ nanosheets with dominant {001} facets,” *J.*, 2009.
- [80] H. Park, W. Kim, H. Jeong, J. Lee, and H. Kim, “Fabrication of dye-sensitized solar cells by transplanting highly ordered TiO₂ nanotube arrays,” *Sol. energy Mater.*, 2011.
- [81] Z. Lin, A. Orlov, and R. Lambert, “New insights into the origin of visible light photocatalytic activity of nitrogen-doped and oxygen-deficient anatase TiO₂,” *J. Phys.*, 2005.
- [82] Y. Qiu, W. Chen, and S. Yang, “Double-layered photoanodes from variable-size anatase TiO₂ nanospindles: a candidate for high-efficiency dye-sensitized solar cells,” *Angew. Chemie*, 2010.
- [83] X. Liu, P. K. Chu, and C. Ding, “Surface modification of titanium, titanium alloys, and related materials for biomedical applications,” 2005.
- [84] M. Sarode, P. Shelke, and Y. Kholam, “Effect of annealing temperature on optical properties of titanium dioxide thin films prepared by sol-gel method,” *J. Mod. ...*, 2011.
- [85] C. Lin, H. Chen, A. Nakaruk, P. Koshy, and C. Sorrell, “Effect of annealing temperature on the photocatalytic activity of TiO₂ thin films,” *Energy Procedia*, 2013.
- [86] T. Peng, X. Xiao, F. Ren, J. Xu, and X. Zhou, “Influence of annealing temperature on the properties of TiO₂ films annealed by ex situ and in situ TEM,” *J. Wuhan*, 2012.
- [87] H. Yin, Y. Wada, T. Kitamura, and S. Kambe, “Hydrothermal synthesis of nanosized anatase and rutile TiO₂ using amorphous phase TiO₂,” *J. Mater.*, 2001.
- [88] M. Suhail, G. Rao, and S. Mohan, “dc reactive magnetron sputtering of titanium- structural and optical characterization of TiO₂ films,” *J. Appl. Phys.*, 1992.
- [89] H. Yoshitake, T. Sugihara, and T. Tatsumi, “Preparation of wormhole-like mesoporous TiO₂ with an extremely large surface area and stabilization of its surface by chemical vapor deposition,” *Chem. Mater.*, 2002.
- [90] Y. Kim, M. Lee, H. Kim, G. Lim, and Y. Choi, “Formation of highly efficient dye-sensitized solar cells by hierarchical pore generation with nanoporous TiO₂ spheres,” *Advanced*, 2009.
- [91] U. Bach, D. Lupo, P. Comte, J. Moser, and F. Weissörtel, “Solid-state dye-sensitized mesoporous TiO₂ solar cells with high photon-to-electron conversion efficiencies,” *Nature*, 1998.
- [92] D. Perednis and L. Gauckler, “Thin film deposition using spray pyrolysis,” *J. electroceramics*, 2005.
- [93] Y. Zheng, E. Shi, S. Cui, W. Li, and X. Hu, “Hydrothermal preparation of nanosized brookite powders,” *Am. Ceram. Soc.*, 2000.

- [94] Y. Tachibana, K. Umekita, and Y. Otsuka, "Performance improvement of CdS quantum dots sensitized TiO₂ solar cells by introducing a dense TiO₂ blocking layer," *J. Phys. D*, 2008.
- [95] F. Iskandar, A. Nandiyanto, and K. Yun, "Enhanced photocatalytic performance of brookite TiO₂ macroporous particles prepared by spray drying with colloidal templating," *Advanced*, 2007.
- [96] P. Ravirajan, S. Haque, and J. Durrant, "The effect of polymer optoelectronic properties on the performance of multilayer hybrid polymer/TiO₂ solar cells," *Adv. Funct.*, 2005.
- [97] G. Messing and S. Zhang, "Ceramic powder synthesis by spray pyrolysis," *J. Am.*, 1993.
- [98] M. Okuya, K. Nakade, and S. Kaneko, "Porous TiO₂ thin films synthesized by a spray pyrolysis deposition (SPD) technique and their application to dye-sensitized solar cells," *Sol. energy Mater. Sol. cells*, 2002.
- [99] H. Afify, S. Nasser, and S. Demian, "Influence of substrate temperature on the structural, optical and electrical properties of ZnO thin films prepared by spray pyrolysis," *J. Mater. Sci. Mater.*, 1991.
- [100] Researchgate, "Principle of FE-SEM operations." Available: https://www.researchgate.net/figure/266912548_fig2_Principle-of-FE-SEM-operations.
- [101] S. Sugapriya, R. Sriram, and S. Lakshmi, "Effect of annealing on TiO₂ nanoparticles," *Opt. J. Light*, 2013.
- [102] LibreTexts, "Powder X-ray Diffraction." Available: https://chem.libretexts.org/Core/Analytical_Chemistry/Instrumental_Analysis/Diffraction_Scattering_Techniques/Powder_X-ray_Diffraction.
- [103] LibreTexts, "Ultraviolet and visible spectroscopy." Available: [https://chem.libretexts.org/Textbook_Maps/Organic_Chemistry_Textbook_Maps/Map%3A_Organic_Chemistry_with_a_Biological_Emphasis_\(Soderberg\)/Chapter_04%3A_Structure_Determination_I/4.4%3A_Ultraviolet_and_visible_spectroscopy](https://chem.libretexts.org/Textbook_Maps/Organic_Chemistry_Textbook_Maps/Map%3A_Organic_Chemistry_with_a_Biological_Emphasis_(Soderberg)/Chapter_04%3A_Structure_Determination_I/4.4%3A_Ultraviolet_and_visible_spectroscopy).
- [104] A. Sedghi and H. N. Miankushki, "The Effect of Drying and Thickness of TiO₂ Electrodes on the Photovoltaic Performance of Dye-Sensitized Solar Cells," vol. 10, pp. 3354–3362, 2015.
- [105] D. Szura, "Synthesis of dye-sensitized solar cells. Efficiency cells as a thickness of titanium dioxide."
- [106] J. Uddin, J. M. M. Islam, S. M. M. Khan, and E. Hoque, "Significant Influence of Annealing Temperature and Thickness of Electrode on Energy Conversion Efficiency of Dye Sensitized Solar Cell : Effect of Catalyst," *Int. Lett. Chem. Phys. Astron.*, vol. 20, no. 1, pp. 78–87, 2014.
- [107] M. Hamadian, V. Jabbari, and A. Gravand, "Dependence of energy conversion efficiency of dye-sensitized solar cells on the annealing temperature of TiO₂ nanoparticles," *Mater. Sci. Semicond.*, 2012.
- [108] M. A. Zulkefle, R. A. Rahman, K. A. Yusof, W. F. H. Abdullah, M. Rusop, and S. H. Herman, "Annealing time dependence of the physical, electrical and pH response characteristics of spin coated TiO₂ thin films," *IOP Conf. Ser. Mater. Sci. Eng.*, vol. 99, p. 12021, 2015.
- [109] N. S. Khalid, S. H. Ishak, and M. K. Ahmad, "Effect of Annealing Time of TiO₂ Thin Film Deposited by Spray Pyrolysis Deposition Method for Dye-Sensitized Solar Cell Application," pp. 647–651, 2015.
- [110] T. Siciliano, M. Di Giulio, M. Tepore, E. Filippa, G. Micocci, and A. Tepore,

- “Effect of thermal annealing time on optical and structural properties of TeO₂ thin films,” *Vacuum*, vol. 84, no. 7, pp. 935–939, 2010.
- [111] “Understanding the Implication of Carrier Diffusion Length in Photovoltaic Cells.”
- [112] N. Park and J. Van de Lagemaat, “Comparison of dye-sensitized rutile-and anatase-based TiO₂ solar cells,” *J. Phys.*, 2000.
- [113] G. Riegel and J. R. Bolton, “Photocatalytic Efficiency Variability in TiO₂ Particles,” *J. Phys. Chem.*, vol. 99, no. 12, pp. 4215–4224, 1995.
- [114] G. Li, C. Richter, R. Milot, and L. Cai, “Synergistic effect between anatase and rutile TiO₂ nanoparticles in dye-sensitized solar cells,” *Transactions*, 2009.
- [115] B. Koo, J. Park, Y. Kim, S. H. Choi, Y. E. Sung, and T. Hyeon, “Simultaneous phase- and size-controlled synthesis of TiO₂ nanorods via non-hydrolytic sol-gel reaction of syringe pump delivered precursors,” *J. Phys. Chem. B*, vol. 110, no. 48, pp. 24318–24323, 2006.